

APF IH-DTL DESIGN FOR THE MUON LINAC IN THE J-PARC MUON G-2/EDM EXPERIMENT

M. Otani, T. Mibe, M. Yoshida, KEK, Oho, Tsukuba, 305-0801, Japan

K. Hasegawa, Y. Kondo, JAEA, Tokai, Naka, Ibaraki, 319-1195, Japan

N. Hayashizaki, Tokyo Institute of Technology, Tokyo, 152-8550, Japan

Y. Iwashita, Kyoto University, Kyoto, 611-0011, Japan

Y. Iwata, NIRS, Chiba, 263-8555, Japan R. Kitamura, University of Tokyo, Hongo, 113-8654, Japan

N. Saito, J-PARC Center, Tokai, Naka, Ibaraki, 319-1195, Japan

Abstract

We have developed an IH-DTL design with an alternative phase focusing (APF) scheme for a muon linac, in order to measure the anomalous magnetic moment and electric dipole moment (EDM) of muons at the Japan Proton Accelerator Research Complex (J-PARC). The IH-DTL accelerates muons from $\beta = v/c = 0.08$ to 0.28 at an operational frequency of 324 MHz. The output beam emittances are calculated as 0.315π and 0.195π mm mrad in the horizontal and vertical directions, respectively, which satisfies the experimental requirement. The design and results are described in this paper.

INTRODUCTION

The low emittance muon beam has been discussed in several scientific fields [1–4]. One of those is the quest for hunting beyond the Standard Model (SM) of elementary particle physics. In the muon anomalous magnetic moment $(g - 2)_\mu$, there is about three standard deviation between the SM prediction and the measured value with a precision of 0.54 ppm [5]. Because it is considered to be due to unknown interaction or particle in the SM, further investigations have been desired. The low emittance muon beam will provide more precise measurement since the dominant systematic uncertainties in the previous experiment resulted from the muon beam dynamics in the muon storage ring.

We are developing a muon linac for the $(g - 2)_\mu$ experiment [6] at Japan Proton Accelerator Research Complex (J-PARC) to realize the low emittance muon beam. Details of the muon linac configuration can be found in [7]. Although conventional linacs adopt Alvarez DTLs after RFQs, an H-mode DTL is employed during the particle velocity $\beta = 0.08$ to 0.28 (4.5 MeV) stage, so as to yield a higher acceleration efficiency.

There are two candidates for the room-temperature H-mode structure. One is an IH structure that works in the TE_{11} -mode, while the other is a CH operated in the TE_{21} -mode [8]. Because the CH and IH structures have comparable acceleration efficiency [9], and because the IH structure is able to be fabricated at lower cost using a three-piece design in which two semi cylindrical shells are attached to a center frame [10, 11], an IH structure is employed. In order to achieve more efficient acceleration, the alternating phase focusing (APF) method is adopted. Although the APF

is limited to a small current beam, as a result of the weak transverse focusing field, it can be applied in a muon linac, because the proposed intensity of the ultra-cold muon beam is very small ($\sim 10^6$ muons per second with 25 bunches).

Following sections in this paper describes the design procedures and results of the APF IH-DTL for the muon linac. You can also refer recently published paper [12] for more detail.

IH DESIGN

In the APF scheme, the gap-to-gap synchronous phases are varied in order to achieve longitudinal and transverse focusing. Because muon has much smaller mass and then the velocity evolution is much rapid compared to the ion with which the APF IH-DTL was recently established [13], the dynamics design is very different to that of ion. In order to find the phase array solution, the beam dynamics are calculated analytically assuming ideal RF field and the synchronous phases for each cell are optimized. Then the IH cavity design is optimized to achieve the ideal RF field by adjusting the geometries other than the cell arrangements. Finally the three-dimensional trajectories in the calculated field are calculated numerically. Details of each step are explained in following sub-sections.

Synchronous Phase Array Optimization

In this step, the particle dynamics are calculated analytically using certain approximations and for a particular synchronous phase array. These calculations are performed using “LINACSapf” [14], with some modifications for the dynamics calculations and the synchronized phase array definition to accommodate the π -mode acceleration, whereas 2π -mode acceleration is assumed in the original code. Details of the approximation method can be found in [12, 14].

The output energy is set to approximately 4 MeV and corresponds to 16 cells. The cavity length is calculated to be approximately 1.3 m. Note that cavities with this length is able to be produced at low cost.

Table 1 shows the optimized phase array results. Gap numbers 1–2, 6–9, 15 and 16 have negative synchronous phases, during which time the beam is longitudinally focused. However, gap numbers 3–5 and 10–14 have positive, during which time the beam is transversely focused. Because the electrostatic focusing effect is stronger in the lower-beta part, the first collection of positive phase groups has a smaller

number of gaps. The output energy is 4.5 MeV and total length is 1.3 m.

Table 1: Cell Parameters for Optimized Phase Array

cell	W [MeV]	β	ϕ [degrees]	cell length [mm]	total length [mm]
1	0.34	0.08	-35.9	29.5	29.5
2	0.43	0.09	-14.9	46.0	75.4
3	0.57	0.10	12.9	54.9	130
4	0.74	0.12	32.9	60.3	191
5	0.92	0.13	15.4	54.4	245
6	1.14	0.15	-13.8	56.0	301
7	1.38	0.16	-31.4	66.4	367
8	1.63	0.17	-44.3	74.1	442
9	1.86	0.19	-18.8	97.2	539
10	2.16	0.20	12.5	108	646
11	2.49	0.21	27.6	106	753
12	2.82	0.23	47.6	116	868
13	3.10	0.24	23.2	94.2	963
14	3.50	0.25	10.8	108	1070
15	3.95	0.27	-34.6	91.5	1160
16	4.30	0.28	-15.6	142	1300
exit	4.50				

IH Cavity Optimization

Because the IH cavity is not axially symmetric, a three-dimensional model is necessary in order to evaluate the electro-magnetic field. In addition, the electro-magnetic field and the resonant frequency depend on the entire structure of the IH cavity, and the detail of the overall structure (including the ridges, etc.) should thus be incorporated in the calculation model. Therefore, the entire IH cavity is modeled using the CST Micro Wave (MW) Studio [15] three-dimensional field solver, in order to calculate the electro-magnetic field. Figure 1 shows the three-dimensional model of the IH cavity in CST MW Studio. The drift tubes and the acceleration gaps are first arranged according to the previously determined optimized parameters shown in Table 1. To optimize the IH cavity, other dimensions, such as the ridges and stems, are optimized. The black and blue lines in Fig. 5 in [12] show the longitudinal electric field along the beam axis before and after these optimizations. The variation in the electric field in the gaps is approximately 10%, excluding the first and last cells.

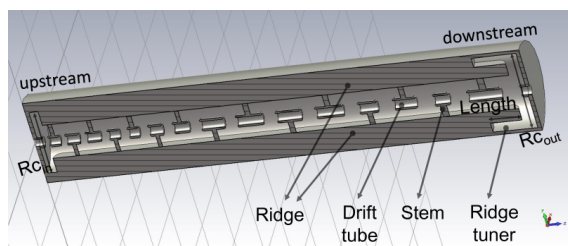


Figure 1: Three-dimensional model of IH cavity in CST MW Studio calculation.

The resonant frequency is tuned to a slightly lower value than the 324-MHz operation frequency, in order to leave

room for the tuner knobs with the inductive tuner installed on the cavity side wall. The quality factor (Q_0) is calculated to be 1.07×10^4 . The effective shunt impedance is calculated to be 92 M Ω /m, and the operation power is required to be 250 kW. The effective shunt impedance is competitive to those of other IH structures given our IH application to relatively higher velocity region.

The maximum surface field is evaluated to be 34 MV/m at the outer surface of the most downstream drift tube, corresponding to 1.9 times the Kilpatrick limit. This value is reasonable based on the experiences in RFQs. Further reduction of the maximum field will be attained through optimization of the chamfered structure at the edge of the drift tube.

Particle Tracking

Next the beam particle trajectory is simulated using the General Particle Tracer (GPT) [16] in which the dynamics are calculated with an embedded fifth order Runge-Kutta driver. The step size is confirmed to be sufficiently small after checking the results with several step sizes. The electric and magnetic fields calculated using CST MW Studio are implemented in the code. The number of simulated particles is 10^5 that corresponds to designed muon beam intensity per bunch. In this size of the current, the space charge effect is negligible.

Top of Fig. 6 in [12] shows the normalized velocity in the x-direction along the beam axis (z) with overwriting of the synchronous phase (ϕ). As shown in the red hatched box in Fig. 6 in [12], the synchronous phases are positive for $z = 130$ – 250 mm and 650 – 1070 mm, where the transverse focusing is implemented. During these periods, the horizontal velocity is decreased.

Bottom of Fig. 6 in [12] shows the normalized velocity in the y-direction along the beam axis. The vertical trajectory is dominated by the finite value of the vertical electric field as shown in the black line in Fig. 2. In order to reduce the additional growth, some conventional solutions, such as the use of drift tube bulges [17], have been considered. However, this approach only reduces the vertical field by a small number of percentage points, as shown in the red line in Fig. 2. It is because the cell length is relatively large (because of the application of the IH structure to yield a higher β region). As a result, no sufficient suppression of the extra growth is achieved using these the additional structures. Because the extra growth is acceptably small and the output beam satisfies the requirement of the J-PARC ($g - 2$) $_{\mu}$ experiment, no additional structures are implemented in this design, so as to avoid additional power loss at these structures.

RESULTS AND CONCLUSIONS

The output beam with the optimized IH design was evaluated. The input beam was obtained from simulations of the surface muon beamline, the ultra slow muon system, and the RFQ [18]. From the results, the normalized root mean

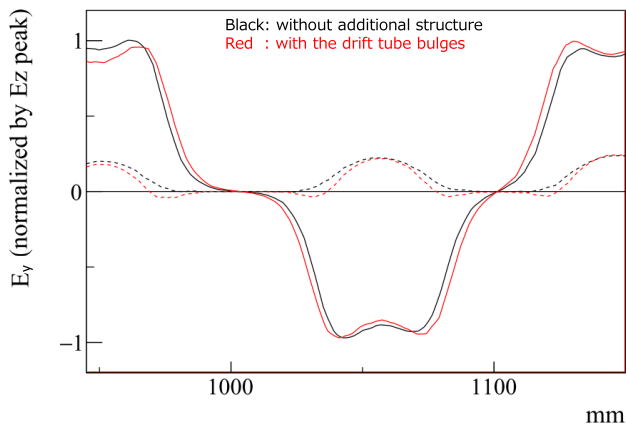


Figure 2: Vertical electric field normalized to the peak value of the axial electric field. Black: field without any additional structures, red: the field with the drift tube bulges.

square (rms) emittances of the input beam were evaluated as 0.297π mm mrad in the x-direction, 0.168π mm mrad in the y-direction, and 0.0181π MeV deg in the z-direction. Because the structure is not periodic due to the APF method and rapidly changing velocity profile, the twiss parameters (α and β) at the IH entrance were scanned in order to obtain a matching condition to the IH, instead of the conventional method solving a periodic solution of the transfer matrix. Based on the scan results, the transport line from the RFQ to the IH was designed using TRACE3D [19], and the beam distributions at the RFQ exit were then transported using PARMILA [20].

Figure 3 shows the acceptance estimated by the GPT code. The acceptance in horizontal and vertical direction slightly differs in the x- and y-direction due to the finite value of vertical electric field as discussed before. The acceptances are sufficiently large compared to the input beam.

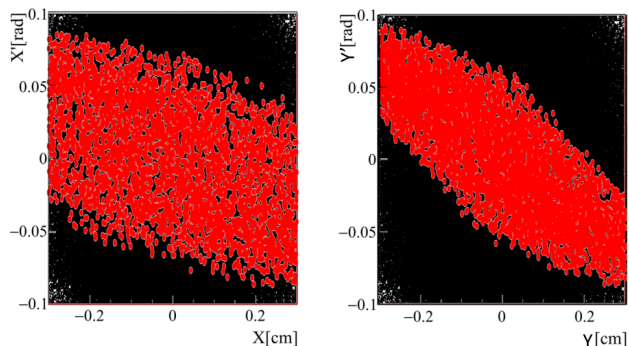


Figure 3: Acceptance estimated by the GPT code. Black points show generated particles and red show the transported particles.

Figure 8 in [12] shows the calculated phase-space distributions of the output beam. The emittance growth was calculated to be 0.018π (6.1%) and 0.027π mm mrad (16%) in the x- and y-directions, respectively. The output beam distributions are improved from those in early work [11] with following reasons; the synchronous phase array was not

optimized in the early work whereas the array was optimized to get smaller emittance growth and higher transmission; the cavity optimization was not sufficient and the axial field distribution has undesirable bump around last cell, which results in the additional energy spread. The transmission efficiency without any selections in output beam was calculated to be 99.9%. The inefficiency comes from the particles which are out of the IH acceptance at injection position. The total transmission including the muon decay loss probability is calculated to be 98.7%, which is sufficient for the experiment.

The beam dynamics in following acceleration structures of DAW [21] are designed with TRACE3D and PARMILA. Figure 4 shows the phase space-space distributions at the DAW exit. It reveals that the emittance growth is only few percents and well within the experimental requirements. Because the RF cavity followed to DAW is a conventional linac structure (disk loaded structure), the emittance growth is expected to be acceptably small. Therefore, the beam emittance will meet the requirement for the experiment.

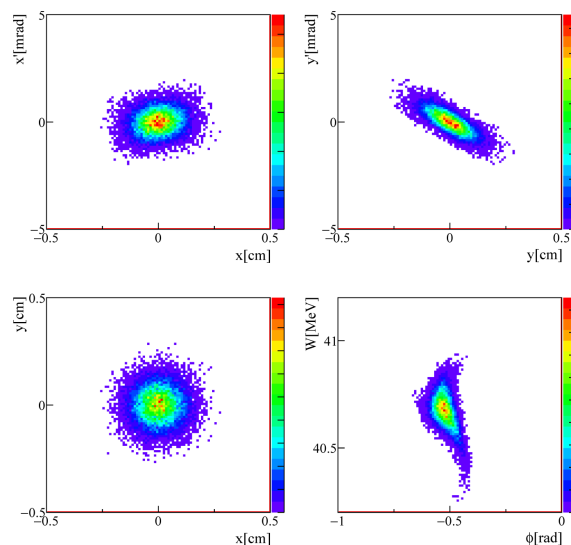


Figure 4: Phase space distributions at DAW exit calculated by PARMILA with using the IH output beam emittance. (top left) the horizontal divergence angle x' vs x , (top right) the vertical divergence angle y' vs y , (bottom left) y vs x , and (bottom right) W vs $\Delta\phi$.

ACKNOWLEDGMENT

The authors are grateful to R. A. Jameson for useful advice on the APF linac and on modifications of the “LINACSapf” code. This work was supported by JSPS KAKENHI Grant Number 15H03666.

REFERENCES

- [1] M. Palmer *et al.*, ICFA Beam Dynamics Newsletter, No.55, 2011.
- [2] Y. Miyake *et al.*, Hyperfine Interact, 216, p.79, 2013.
- [3] M. Bogomilov *et al.*, JINST 7, P05009, 2012

- [4] S. Artikova *et al.*, PASJ2013 Proc. (Nagoya, Japan, 2013), SAP045.
- [5] G.W. Bennett *et al.*, Phys. Rev. D73, 072003, 2006.
- [6] J-PARC E34 conceptual design report, 2011. (unpublished)
- [7] M. Otani *et al.*, Proc. of IPAC2016. (Busan, Korea, 2016), TUPMY02.
- [8] S.S. Kurennoy *et al.*, Phys. Rev. ST Accel. Beams 14, 110101, 2011.
- [9] U. Ratzinger, CERN Yellow Report No.2005-003 p.351, 2005.
- [10] E. Nolte *et al.*, Nucl. Instru. Meth. 158, 311, 1979.
- [11] N. Hayashizaki and M. Yoshida, PASJ2014 Proc. (Aomori, Japan, 2014), SUP043.
- [12] M. Otani *et al.*, “Interdigital H-mode drift-tube linac design with alternative phase focusing for muon linac”, Phys. Rev. Accel. Beams, 19, 040101, 2016.
- [13] Y. Iwata *et al.*, Nucl. Instr. Meth. A569, 685, 2006.
- [14] R.A. Jameson, arXiv:1404.5176[physics.acc-ph]
- [15] CST Studio Suite, Computer Simulation Technology (CST). [<https://www.cst.com/products/CSTMWS>]
- [16] General Particle Tracer, Pulsar Physics. [<http://www.pulsar.nl/gpt/>]
- [17] S.S. Kurennoy *et al.*, Phys. Rev. ST Accel. Beams 15, 090101, 2012.
- [18] Y. Kondo *et al.*, Proc. of IPAC2015, 2015, THPF045, 2015
- [19] K.R. Crandall and D.P. Rustoi, Los Alamos Report, No. LA-UR-97-886, 1997.
- [20] Los Alamos Accelerator Code Group (LAACG), LANL, Los Alamos, [<http://www.laacg.lanl.gov>].
- [21] M. Otani *et al.*, PASJ2015 Proc. (Tsuruga, Japan, 2015), WEOM02.